Met. Mater. Int., Vol. 18, No. 6 (2012), pp. 1023~1027
doi: 10.1007/s12540-012-0483-2

Studies on the Application of Laser Surface Texturing to Improve the Tribological Performance of AlCrSiN-Coated Surfaces

Bom Sok Kim[1], Woo Yooung Chung[2], Meung-Ho Rhee[2], and Sang-Yul Lee[1,*]

[1]Center for Surface Technology and Applications, Korea Aerospace University,
76 Hang Gong Dae-ro, Deogyang-gu, Goyang-si, Gyeonggi-do 412-791, Korea
[2]Korea Automotive Technology Institute, Yongjeong-ri 74, Pungse-myeon, Cheonan-si,
Chungcheongnam-do 330-912 Korea

(received date: 20 December 2011 / accepted date: 23 February 2012)

Recently, laser texturing has received lots of attention for improving the tribological performance of various surfaces, and this laser texturing of surfaces could be applied to improve the tribological performance of PVD coated surfaces. In this work two different patterns of laser surface texturing were performed on H13 substrate, and PVD AlCrSiN coatings with various N_2 contents were made by unbalanced magnetron sputtering on the textured H13 specimens. The coating characteristics such as crystalline structure, surface morphology, hardness, and friction coefficient of the coatings as a function of the N_2 partial pressure were investigated by X-ray diffraction (XRD), atomic force microscopy (AFM), microhardness tester, and wear test. Synthesis of the AlCrSiN thin films containing various N_2 contents was successful using the unbalanced magnetron sputtering process. A dense and compact microstructure, as well as a very smooth surface, were observed from the synthesized thin films, which could be attributed to the addition of Si into the AlCrN films, producing an amorphous phase in the films. Also the hardness of the AlCrSiN films increased with increasing N_2 partial pressures and the maximum hardness of approximately 33 GPa was measured from the AlCrSiN film synthesized with N_2 partial pressures of 0.16 Pa. From the wear tests against an Al_2O_3 counterpart ball at room temperature without lubrication, the average friction coefficient of the non-textured AlCrSiN films of 0.42 was decreased to 0.38 and 0.36 for dimple-textured and honeycomb-textured AlCrSiN films, respectively. Laser surface texturing on the AlCrSiN films reduced the friction coefficients by approximately more than 15%, and further improvement on the tribological performance of the textured surfaces could be possible by optimizing the honeycomb-textured surfaces.

Key words: laser surface texturing, thin films, sputtering, wear, hardness test

1. INTRODUCTION

Much attention has been paid to surface texturing, which can induce an improvement of tribological properties by enhancing lubrication in many applications including cylinder liners [1-4], storage devices [5,6], MEMS [7], and toolings [8-12]. It was reported that depressions made on these surfaces act not only as features to trap wear particles, reducing the ploughing component of friction [11,13] but also as reservoirs for liquid lubricants, capable of feeding the lubricant between the sliding surfaces [10,11,13-16].

Surface texturing has recently been demonstrated by various manufacturing techniques such as indentation with hard materials [17,18], ion etching [19], abrasive jet machining [10], lithography [20], and Laser Surface Texturing (LST) [8,21,22]. Out of all these techniques, however it is generally accepted that LST offers the most promising process as it is very fast, environmentally-friendly, and can easily control the shape and size of the microdimples.

While AlCrN coatings were reported to show a low friction coefficient, low wear rate, and excellent cutting performance in high speed dry machining [23-25], the addition of Si into AlCrN coatings to make quaternary AlCrSiN coatings induced beneficial modification in terms of the grain size, phase composition and mechanical properties [26,27]. In AlCrSiN coatings, an amorphous silicon nitride phase formed along the grain boundaries [26] to make these coatings not only more wear resistant [28], but also more oxidation resistant than AlCrN coatings [29,30]. Due to the excellent mechanical properties and oxidation resistance, AlCrSiN coatings have received much attention for wear applications at high temperature, such as dry cutting tools.

In this study, hard AlCrSiN films were coated on surfaces

*Corresponding author: sylee@kau.ac.kr

treated by laser surface texturing with different patterns, and the influence of surface texturing in terms of the wear behaviors of the AlCrSiN coating were evaluated. The aim of this work was to make a preliminary investigation on the feasibility of combining surface texturing and hard coating to further improve the tribological properties in a dry sliding condition.

2. EXPERIMENTAL PROCEDURES

In this work the laser texturing was accomplished by Marking Laser System (YLP-20, 20W) and detailed operating conditions are summarized in Table 1. Two types of LST patterns were made on the H13 steel substrate and their shape and dimensions are presented in Fig. 1. After the LST process, the spatters formed during the LST process were polished away using SiC #400 papers and equally spaced patterns with dimples and honeycombs were produced over the entire sample surface (Fig. 1).

AlCrSiN films of approximately 2 μm were deposited on silicon (100) wafer for the coating analysis, and laser surface textured AISI H13 steel by closed field unbalanced magnetron sputtering with vertical magnetron sources (see Fig. 2).

Table 1. Laser specifications and operating conditions

Model	YLP-20
Mode	Single
Energy per pulse (20 kHz)	1mJ
Pulse Width	100ns
Pulse Repetition Rate	20-80 kHz
Laser Type	Fiber Laser
Output Power	20W
Wave Length	1,064 nm

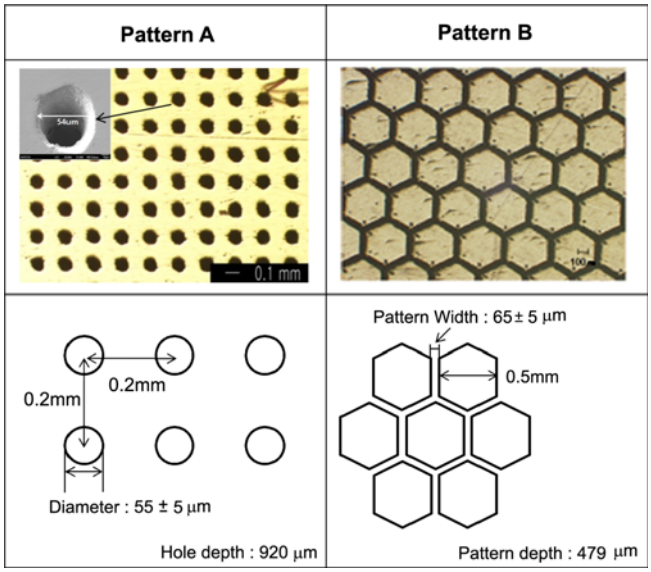

Fig. 1. Two LST patterns used in this work : types and dimensions.

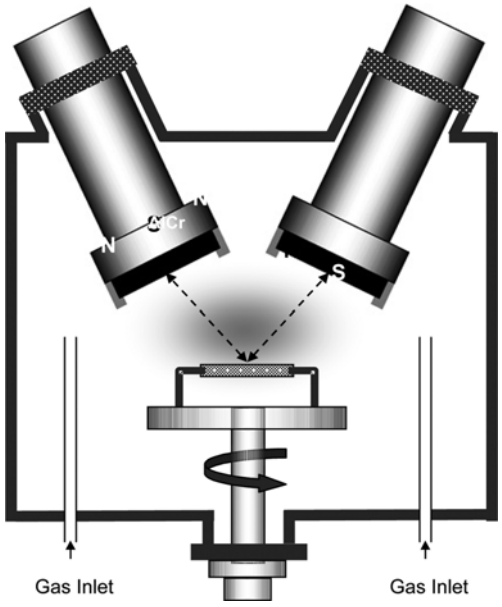

Fig. 2. Schematic diagram of the closed field unbalanced magnetron sputtering with vertical magnetron sources.

In this apparatus, two magnetron sources installed with a metallic AlCr segment target (Al:Cr=50:50 volume ratio) and Si targets were mounted on the top part of the deposition chamber and the polarity of magnets between two magnetron sources was arranged oppositely in order to form a closed magnetic field. This apparatus has an advantage in that high-level ion bombardments are continuously provided during the deposition process, as dense plasma is maintained on the substrate by the closed trap of the magnetic field lines between the two magnetron sources. Prior to the films' deposition, the base pressure of the sputtering chamber was pumped down to less than 2.0×10^{-3} Pa and pre-sputtering was carried out by placing a shutter between the targets and substrate for ten minutes, to clean the target surface, at the Ar pressure of 0.4 Pa. After target cleaning, the deposition of films was performed in an Ar-N_2 mixture atmosphere by fixing theAr pressure at 0.4 Pa and by varying N_2 pressure between 0.04 and 0.16 Pa. In the deposition conditions of films, the target powers of both targets were maintained at pulsed DC 0.5 kW (frequency: 25 kHz, duty: 70%). Other conditions such as substrate bias voltage, distance of target-to-substrate, deposition temperature and substrate rotation speed were fixed to -100 V, 80 mm, 100 °C, respectively.

The chemical composition of the coatings was determined by glow discharge optical emission spectroscopy (GDOES: LECO GDS 850A) and the crystal phases were characterized by X-ray diffraction (XRD: D/max2200) with Cu Kα radiation (λ=0.15418 nm). For the AlCrSiN coatings, the bonding status was analyzed by X-ray photoelectron spectroscopy (XPS: VG Multilab ESCA 2000) with a monochromatic Al

Kα radiation (1481 eV). The hardness was measured using a microhardness tester (Fisherscope: H100CXYp) instrument with a load of 50 mN. The surface and cross sectional morphologies were investigated by atomic force microscopy (AFM) and field emission scanning electron microscopy (FE-SEM: HITACHI S-4700). The wear property of coatings was evaluated using a ball-on-disk type tribometer with a 9.25 mm diameter Al_2O_3 ball as a counterpart material. The test was performed in the room atmosphere temperature of 25 °C and relative humidity of 45% without lubrication under an applied normal load of 5.0 N. The sliding velocity was 0.25 m/s with a wear track diameter of 35 mm and the total sliding distance was 1000 m. During the test, the variation of friction coefficient on the sliding distance was measured and the wear track formed on the specimen after the wear test was examined by scanning electron microscopy.

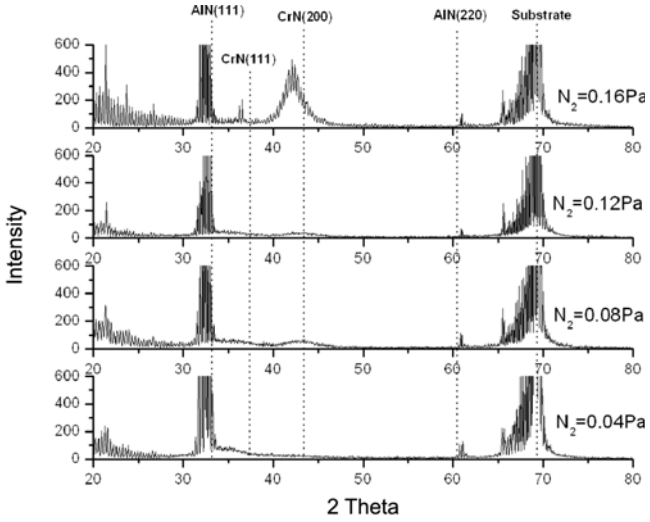

Fig. 3. X-ray diffraction patterns of the AlCrSiN films synthesized with various N_2 partial pressure.

3. RESULTS AND DISCUSSION

The chemical compositions of the films determined by GDOES analysis are listed in Table 2. With increasing N_2 partial pressures from 0.04 to 0.16 Pa, the nitrogen content in the films increased almost linearly as a function of the N_2 partial pressures, whereas the atomic ratios of Al/Al+Cr+Si and Cr/Al+Cr+Si were maintained at nearly constant values of approximately 0.59 and 0.25, respectively as AlCr target power was kept constant during the whole deposition process. The Si/Al+Cr+Si ratio increased as the N_2 partial pressure increased.

Figure 3 shows the X-ray diffraction patterns of the AlCrSiN films deposited at the various N_2 partial pressures. XRD patterns in Fig. 3 revealed the presence of a strong AlN phase which could be assigned to cubic B1 NaCl structure. The AlCrSiN films have a strong preferred orientation of (111), and this peak has been shifted to a lower diffraction angle probably due to the extensive addition of Cr and Si to the AlN phase. In the films grown with the higher N_2 pressure of 0.16 Pa, a CrN (200) peak was observed from the AlCrSiN films while with lower N_2 pressure, broad and low intensity peaks were observed which indicates the formation of an amorphous phase. It was also noticed that the CrN (200) peak observed from the AlCrSiN films synthesized with the nitrogen partial pressure of 0.16 Pa was shifted more toward a lower diffraction angle, probably due to the high solid solution characteristics of the CrN phase.

The cross-sectional and surface morphologies of the AlCrSiN films synthesized with various nitrogen partial pressures are shown in Fig. 4. Compared with those of AlCrN coatings reported previously [31], the addition of Si into the AlCrN films made the film microstructure more dense and smooth. This could probably be due to the formation of an amorphous phase by the addition of Si element into the films, and with decreasing N_2 partial pressures, their microstructure became increasingly denser and more amorphous, which is consistent with the results from XRD analysis as shown in Fig. 3.

Figure 5 shows the hardness curves of the films synthesized at the various N_2 partial pressures. These were measured using a nanoindenter with a continuous stiffness measurement (CSM) technique, which applies a continuous loading-unloading indentation with a frequency of 45 Hz. The intrinsic hardness of the films, not including the substrate effect, could be generally obtained from a plateau region of the hardness curve measured by the CSM technique [32]. Average values obtained at an indentation depth ranging between 75 and 125 nm were measured. The hardness of the AlCrSiN films increased with increasing N_2 partial pressures and the maximum hardness of approximately 33 GPa was measured from the AlCrSiN film synthesized with N_2 partial pressures of 0.16 Pa This value was much higher than that of binary AlN [31] (H= 23GPa). The hardness enhancement for the AlCrSiN films could be primarily caused by the solid

Table 2. Chemical compositions of the films determined by GDOES analysis

N_2 partial pressure (Pa)	Al (at.%)	Cr (at.%)	Si (at.%)	N (at.%)	Al/Al+Cr+Si	Cr/Al+Cr+Si	Si/Al+Cr+Si	Total
0.04	36.7	16.5	9.3	37.5	0.59	0.26	0.149	100
0.08	35.3	15.1	9.4	40.2	0.59	0.25	0.157	100
0.12	32.2	14.1	9.1	44.6	0.58	0.25	0.164	100
0.16	29.4	11.3	9.5	49.8	0.59	0.23	0.189	100

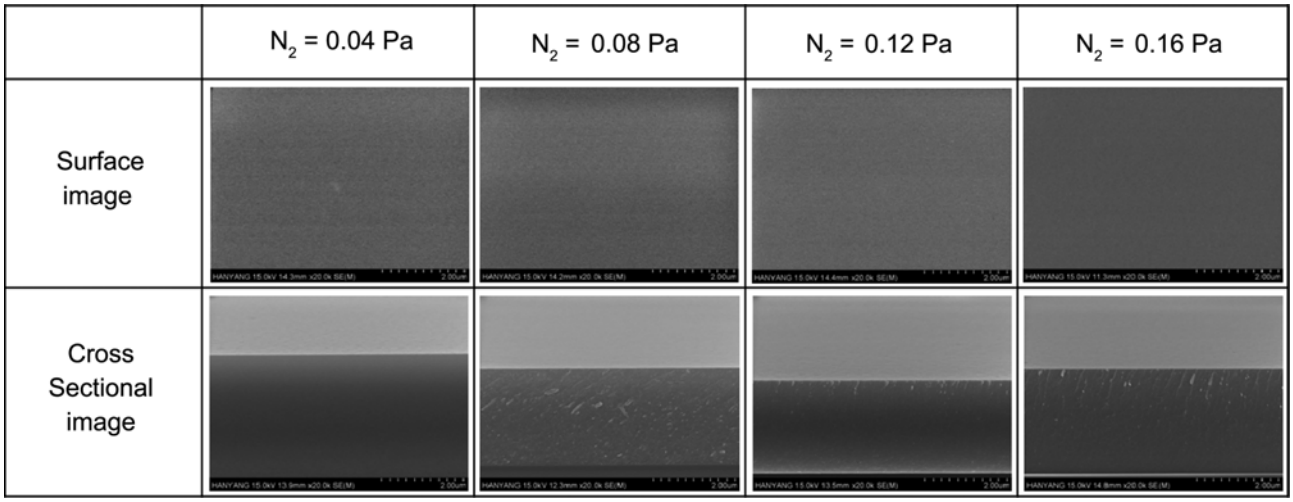

Fig. 4. Cross-sectional and surface morphologies of the AlCrSiN films.

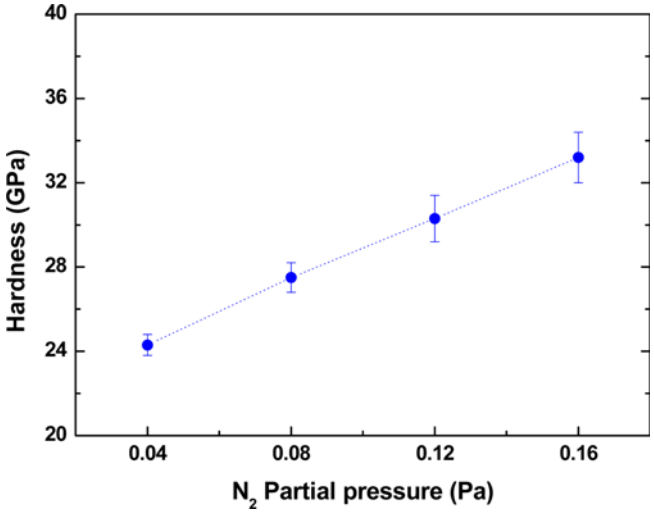

Fig. 5. Hardness of the AlCrSiN films as a function of N_2 partial pressures.

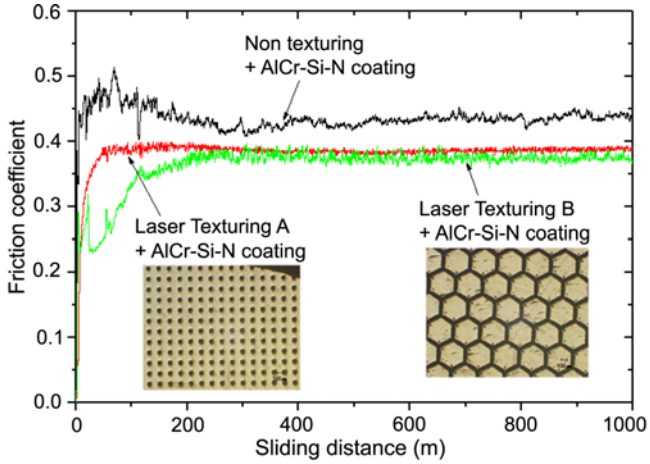

Fig. 6. Friction coefficient curves of the laser surface textured AlCrSiN films.

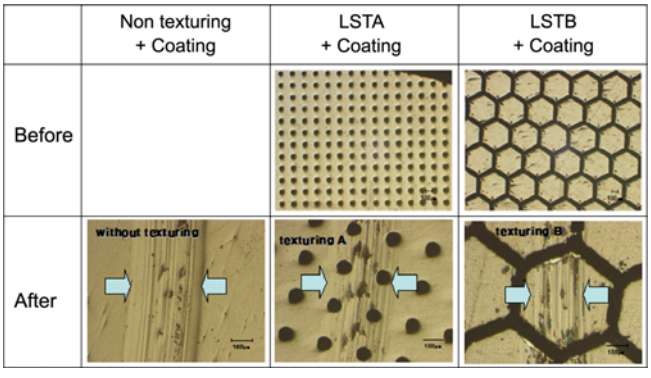

Fig. 7. Micrographs of wear tracks produced on the laser surface textured AlCrSiN films.

solution hardening. As a solid solution in the (AlCr)N films is generated, lattice distortion inhibits the mobility of the dislocations, inducing a hardness enhancement. Also, the AlCrSiN films are expected to have a similar nanocomposite structure with TiAlSiN films [33], consisting of crystalline (AlCr)N phase and amorphous Si_3N_4 phase.

From the wear tests against an Al_2O_3 counterpart ball at room temperature, the friction coefficient curves of the laser surface textured AlCrSiN films deposited on the AISI H13 steel substrate under 0.16 Pa N_2 partial pressures (films with the highest microhardness of 33 GPa) are shown in Fig. 6. All films have a similar film thickness of approximately 2.0 μm. The average friction coefficient of the non-textured AlCrSiN films of 0.42 was decreased to 0.38 and 0.36 for dimple-textured and honeycomb-textured AlCrSiN films, respectively. Laser surface texturing on the AlCrSiN films reduced the friction coefficients by more than 15%.

After wear tests against a counterpart Al_2O_3 ball, we obtained micrographs of wear tracks produced on the laser surface

textured AlCrSiN films, as shown in Fig. 7. During the wear test, all the films showed an abrasive wear and the macro-failures of films were not observed from the wear tracks. However, a slight variation in the width of the wear tracks was observed, and the film with honeycomb-textured films showed the minimum wear width of approximately 250 μm, suggesting the ideal surface texturing could be obtained from the honeycomb-type surfaces.

4. CONCLUSIONS

(1) In this work AlCrSiN coatings with various N_2 contents were successfully synthesized by unbalanced magnetron sputtering, and the AlCrSiN coatings consisted mainly of the crystalline (AlCr)N and amorphous phases. The cross-sectional and surface morphologies of the AlCrSiN films synthesized with various nitrogen partial pressures showed a dense and compact microstructure as well as a very smooth surface, which could be due to the addition of Si into the AlCrN films, producing the formation of an amorphous phase in the films.

(2) The hardness of the AlCrSiN films increased with increasing N_2 partial pressures. The maximum hardness of approximately 33 GPa was measured from the AlCrSiN film synthesized with N_2 partial pressures of 0.16 Pa and this value was much higher than that of binary AlN (H=23GPa).

(3) From the wear tests against an Al_2O_3 counterpart ball at room temperature, the average friction coefficient of the non-textured AlCrSiN films of 0.42 was decreased to 0.38 and 0.36 for dimple-textured and honeycomb-textured AlCrSiN films. Laser surface texturing on the AlCrSiN films reduced the friction coefficients by approximately more than 15%, and further improvement on the tribological performance of the textured surfaces could be possible by optimizing the honeycomb-textured surfaces.

ACKNOWLEDGMENTS

This research was supported by a grant from the Fundamental R&D Program for Core Technology of Materials funded by the Ministry of Knowledge Economy, Republic of Korea.

REFERENCES

1. Y. R. Jeng, *Tribol. Trans.* **39**, 354 (1996).
2. E. Willis, *Wear* **109**, 351 (1986).
3. J. H. Jang, B. D. Joo, J. H. Lee, and Y. H. Moon, *Met. Mater. Int.* **15**, 903 (2009).
4. W. J. Kim, J. G. Kim, S. J. Park, and K. R. Lee, *Met. Mater. Int.* **11**, 473 (2005).
5. R. Ranjan, D. N. Lambeth, M. Tromel, P. Goglia, and Y. Li, *J. Appl. Phys.* **69**, 5745 (1991).
6. L. Zhou, K. Kato, G. Vurens, and F. E. Talke, *Tribol. Int.* **36**, 269 (2003).
7. K. Komvopoulos, *J. Adhes. Sic. Technol.* **17**, 477 (2003).
8. G. Dumitru, V. Romano, H.P. Weber, Y. Gerbig, and E. Pfluger, *Appl. Phys. A* **70**, 485 (2000).
9. I. E. Ostfildern, *Tribology and Lubrication Eng.*, **1**, 329 (2004).
10. M. Wakuda, Y. Yamauchi, S. Kanzaki, and Y. Yasuda, *Wear* **254**, 356 (2003).
11. P. Andersson, J. Koskinen, S. Varjus, Y. Gerbig, H. Haefke, S. Georgiou, B. Zhmud, and W. Buss, *Wear* **262**, 369 (2007).
12. L. M. Vilhena, M. Sedlaček, B. Podgornik, J. Vižintin, A. Babnik, and J. Možina, *Tribol. Int.* **42**, 1496 (2009).
13. U. Pettersson and S. Jacobson, *Tribol. Lett.* **17**, 553 (2004).
14. A. Ronen, I. Etsion, and Y. Kligerman, *Tribol. Trans.* **44**, 359 (2001).
15. X. Wang, K. Adachi, K. Otsuka, and K. Kato, *Appl. Surf. Sci.* **253**, 1282 (2006).
16. Y. S. Hong and S. Y. Lee, *Met. Mater. Int.* **14**, 33 (2008).
17. Y. G. Schneider, *Precis. Eng.* **6**, 219 (1984).
18. U. Petterson and S. Jacobson, *Tribol. Int.* (2005).
19. X. Wang, K. Kato, K. Adachi, and K. Aizawa, *Tribol. Int.* **36**, 189 (2003).
20. U. Pettersson and S. Jacobson, *Tribol. Int.* **36**, 857 (2003).
21. I. Etsion, *J. Tribol.* **127**, 248 (2005).
22. A. Hoppermann, M.Kordt, *O+P O¨lhydraulik und Pneumatik Vereinigte Fachverlage Mainz* **46**, (2002).
23. B. C. Schramm, H. Scheerer, H. Hoche, E. Broszeit, E. Abele, and C. Berger, *Surf. Coat. Technol.* **188-189**, 623 (2004).
24. P. H. Mayrhofer, H. Willmann, and A. E. Reiter, *Surf. Coat. Technol.* **202**, 4935 (2008).
25. X. Z. Ding, A. L. K. Tan, X. T. Zeng, C. Wang, T. Yue, and C. Q. Sun, *Thin Solid Films* **516**, 5716 (2008).
26. J. L. Endrino, S. Palacín, M. H. Aguirre, A. Gutiérrez, and F. Schäfers, *Acta Mater.* **55**, 2129 (2007).
27. J. Soldán, J. Neidhardt, B. Sartory, R. Kaindl, R. Čerstvý, P. H. Mayrhofer, R. Tessadri, P. Polcik, M. Lechthalter, and C. Mitterer, *Surf. Coat. Technol.* **202**, 3555 (2008).
28. D. Rafaja, C. Wüstefeld, M. Dopita, M. Růžička, V. Klemm, G. Schreiber, D. Heger, and M. Šíma, *Surf. Coat. Technol.* **201**, 9476 (2007).
29. D. B. Lee, T. D. Nguyen, and S. K. Kim, *Surf. Coat. Technol.* **203**, 1199 (2009).
30. S. K. Tien, C. H. Lin, Y. Z. Tsai, and J. G. Duh, *Surf. Coat. Technol.* **202**, 735 (2007).
31. S. Y. Lee and G. S. Kim, *Surf. Coat. Technol.* **201**, 4361 (2006).
32. S. Y. Lee, G. S. Kim, J. H. Hahn, and S. Y. Lee, *Surf. Coat. Technol.* **171**, 91 (2003).
33. G. S. Kim, B. S. Kim, S. Y. Lee, and J. H. Hahn, *Thin solid Films* **506-507**, 128 (2006).